

SYNTHESIS, STUDY OF ELECTRICAL, THERMAL BEHAVIOR OF POLYANILINE-POLYSTYRENE SULPHONIC ACID COMPOSITE

G. MURTAZA^{ab*}, I. AHMAD^a

^aDepartment of Physics, Bahauddin Zakariya University, Multan 60800 Pakistan

^bDepartment of Physics, GC University Faisalabad, Layyah Campus, Layyah 31200, Pakistan.

We report the synthesis, electrical and thermal properties of Polyaniline-Polystyrene sulphonic acid (PAni-PSSA) composite. The incorporation of Polyaniline in Polystyrene sulphonic acid (PSSA) is clearly revealed by the Fourier transform infrared spectroscopy (FTIR). Differential scanning calorimeter (DSC) thermograph shows three step transitions in Polyaniline-Polystyrene sulphonic acid composites. Frequency dependent dielectric constant, dielectric loss and ac conductivity are studied in the range 1Hz to 3GHz. The ac conductivity shows a plateau like behavior in the low frequency region and it shows dispersion in the high frequency region. The variation of dielectric constant and tangent loss is the net effect of external and internal applied ac field. The value of real and imaginary part of dielectric constant decreased with increasing frequency which indicates that the major contribution to the polarization comes from orientation polarization.

(Received August 17, 2016; Accepted November 22, 2016)

Keywords: Fourier transform infrared spectroscopy (FTIR); Differential scanning calorimeter (DSC); Dielectric constant; Thermo gravimetric analysis (TGA).

1. Introduction

The study of conducting polymers was first introduced by Shirakawa *et. al.* in 1977 [1]. The chemical and physical properties of the conducting polymers which appear from their unique π -conjugation have attracted much attention [2]. Conducting polymers are used in advanced applications like gas sensors, plastic batteries, electrochromic displays, supercapacitors, electronics, drug delivery, corrosion protection, EMI shielding, nonlinear optics, gas separation membranes, humidity sensors and enzyme immobilization [1-5]. The poor mechanical properties of the conducting polymers have limited their applications but some have excellent mechanical and thermal properties [6]. The electrical conductivity of these polymers lies between 10^{-5} S/cm and 10^2 S/cm while the insulators which are commonly used have conductivity below 10^{-12} S/cm [7]. Polyaniline (PAni) is considered as one of the best materials that can be used in electronics due to its processability and stability. The most promising organic conducting polymers PAni emerged due to its low cost, good environmental stability, high polarization yield and moderate conductivity [8]. The important green chemistry is based on the preparation of multifunctional conducting polymers and their derivatives by oxidative polymerization [9]. The foremost work on the preparation of conducting polymer "Aniline Black" was published in 1862 [10]. It was synthesized at that time by the anodic oxidation of aniline and it changes color upon applying a potential that is why it is laterally known as electrochromic material and its electrical properties were not measured at that time [11]. MacDiarmid reported first time that aniline is an acid aqueous solution in 1985 which can be oxidized chemically by using an oxidant ammonium peroxydisulfate (APS) to obtain green powder of PAni having good conductivity [12, 13]. In this paper, we have synthesized and studied the electrical and thermal behavior of PAni-PSSA composite.

*Corresponding author: mrkhichi@gmail.com

2. Experimental

2.1 Materials

All the chemicals which are used in this study are of analytical grade. Aniline monomers having 99% purity are of Sigma Aldrich and polystyrene sulphonic acid (PSSA) is purchased from Alfa Aesar (wt 30% water solution, Mw75000). Ammonium persulfate (APS) is obtained from Fluka.

2.2 Synthesis of water soluble PANi-PSSA

The water soluble PANi-PSSA is prepared by chemical oxidative polymerization method in which ammonium persulfate (APS) can be used as an oxidant [14, 15]. In this process 7.5 g of PSSA is added into 20 ml deionized water and put it into a flask then 0.2 ml of aniline is added and the mixture is kept on stirring for one hour. Drop 10 ml of aqueous solution of ammonium persulfate (APS) (0.05 g/ml) into the mixture. After it the mixture is stirred for half an hour, and stood for another 12 hours. Finally the resultant is precipitated and washed many times with acetone and deionized water. Dry the powder under vacuum at room temperature for 48 hours to obtain a dark-green powder of Polyaniline-Polystyrene sulphonic acid.

2.3 Preparation of sample and Measurements

In order to measure the electrical properties, the material was grounded with the help of mortar and pestle; the powder was pressed into pellets under the load of (~60 KN) by using the Paul-Otto weber Hydraulic press. The diameter of the pellet was 8 mm while its thickness was 3 mm. The dielectric measurements were taken with the help of Agilent 4287A and the measured frequency range was 1 Hz to 3 GHz. TG and DSC were measured on STA 409 Cd and the heating rate was kept at 10 °C/min.

2.4 Dielectric evaluation

The complex dielectric permittivity can be written as $\varepsilon^*(\omega) = \varepsilon'(\omega) - j\varepsilon''(\omega)$ where ε' and ε'' are the real and imaginary part of the permittivity respectively, with $j = \sqrt{-1}$. The following parameters such as equivalent capacitance (C), dissipation factor (D) can be used to calculate the dielectric constant with the help of Agilent meter at different frequencies. The commonly employed relations are as under,

$$\varepsilon'(\omega) = c(\omega) \frac{d}{A\varepsilon_0}, \quad (1)$$

$$\varepsilon''(\omega) = \varepsilon'(\omega) \tan \delta, \quad (2)$$

$$\sigma_{ac}(\omega) = \omega\varepsilon_0\varepsilon''(\omega) = \omega\varepsilon_0\varepsilon'(\omega)\tan \delta, \quad (3)$$

where σ_{ac} , d , A , δ , D ($\tan\delta$) represent ac conductivity, thickness, effective area of the sample, phase angle and dissipative factor respectively. The electrical properties of a polymer composite cannot be described by the complex permittivity. It is essential to calculate the electric modulus $M^*(\omega)$ which is very helpful for the detail study of the electrical properties of a polymer composite. The real and imaginary part of the electric modulus $M^*(\omega)$ can be calculated from $\varepsilon^*(\omega)$ [14],

$$M^*(\omega) = \frac{1}{\varepsilon^*(\omega)} = M' + jM'', \quad (4)$$

where the real part of electric modulus $M^*(\omega)$ is,

$$M'(\omega) = \frac{\varepsilon'}{\varepsilon'^2 + \varepsilon''^2}, \quad (5)$$

and the imaginary part of electric modulus $M''(\omega)$ is as under,

$$M''(\omega) = \frac{\epsilon''}{\epsilon'^2 + \epsilon''^2}, \quad (6)$$

The complex dielectric permittivity $\epsilon^*(\omega)$ is a factor that lies between alternating electric field $\vec{E}(\omega)$ and polarization (\vec{P}) of the material [15, 16]. Polarization relation can be written as,

$$\vec{P}(\omega) = (\epsilon^*(\omega) - 1) \epsilon_0 \vec{E}(\omega), \quad (7)$$

where ϵ_0 , ω are the permittivity of the free space and angular frequency, respectively. The data for complex permittivity depends on the physical properties like pressure, temperature, frequency and composition of the materials. In the light of statistical mechanics both ϵ' and ϵ'' have important physical meaning; where ϵ' , ϵ'' stands for the energy stored per cycle and for the energy loss per cycle, respectively. The complex dielectric permittivity is related to the free oscillation in an ac electric field as described by Havriliak-Negami relation [17-19].

3. Results and Discussions

3.1 Frequency dependent electrical properties of PANi-PSSA

The maximum value of dielectric constant appears at low frequency is the result of interfacial dislocation pile up, grain boundary defect and oxygen vacancies etc. Dielectric constant varies with frequency depicts the dispersion due to Maxwell Wagner interfacial polarization that is in agreement with Koop's phenomenology theory [20-23]. The data shows that the dispersion of the dielectric constant at low frequency comes from the grain boundary and at high frequency it comes from the grains. The value of the real and imaginary part of dielectric constant decreases with the increase of frequency, the variation of the real and imaginary part of dielectric constant with frequency is shown in Fig. 1(a). Electrons are distributed around the nuclei evenly in the absence of an electric field but at the application of electric field; electron cloud is displaced from the nuclei in the direction opposite to the applied electric field. As a consequence, the separation between the negative and positive charge take place and the molecule behave like an electric dipole [24]. The loss in dielectric value arises from the inability of polarization in a molecule to follow the rate of change of the oscillating applied electric field. The dielectric constant values of PANi-PSSA decreases with increasing frequencies. The decrease in dielectric constant with frequency is due to either the lag of dipole oscillations behind those of the applied ac electric field at high frequencies or due to more need of thermal energy to disturb the ordered dipoles at higher frequencies of the applied field [25]. At low frequency, the values of the real dielectric constant of PANi-PSSA show the energy stored ability in the composite is high which is decreasing with the increase of frequency. The dielectric material with a heterogeneous structure can be imagined as a structure consists of well conducting grains separated by highly resistive thin layers called grain boundaries. In this case, the applied voltage acts on the small particles (grains) and a space charge polarization is build up at grain boundaries. Space charge polarization is due to the conductivity of the grains and the presence of the free charges at the grain boundary. Koop proposed that the effect of grain boundaries is predominant at low frequencies. The high value of the dielectric constant is the result of the thinner grain boundaries [26-30].

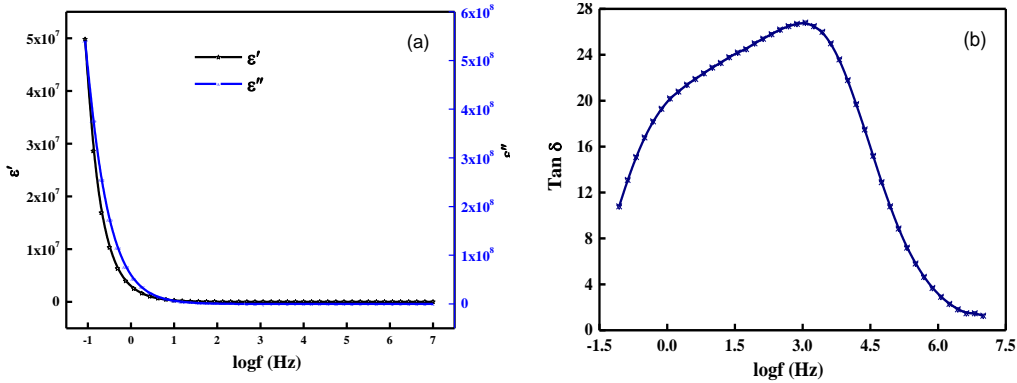


Fig. 1 Frequency dependent dielectric constant for PANi-PSSA
(a) Real and Imaginary part (b) dielectric loss.

The decrease in the imaginary part of dielectric constant with increase in frequency agrees well with the Debye relaxation process. The value of imaginary part of dielectric constant attains a maximum value then it decreases due to the power loss and more energy dissipation takes place in the composite [31, 32]. From the structural point of view, the dielectric relaxation involves the orientation polarization which in turn depends upon the molecular arrangement of dielectric to material. So at high frequency the rotational motion of the polar molecules of dielectric is not sufficiently rapid for the attainment of equilibrium with the field, hence dielectric constant seems to be decreasing with increasing frequency. Fig. 1 (b) shows the Tan loss of PANi-PSSA, it has a high value as compared to conducting polymers. The condition for observing a maximum in the dielectric losses of a dielectric material is given by $\omega_{\max}\tau = 1$. Where, $\omega_{\max} = 2\pi f_{\max}$ and the symbol (τ) is the relaxation time that represents the jumping probability per unit time ‘p’ for the three type polarization. The electric modulus is just the reciprocal of complex dielectric permittivity.

$$M^*(\omega) = \frac{1}{\epsilon^*}, \tag{8}$$

Fig. 2 shows the frequency dependence of real and imaginary part of electric modulus of PANi-PSSA. At high frequency, the real part of electric modulus M' shows dispersion while at low frequency it tends to zero which shows the low contribution of electrode polarization to M' . At high frequency dielectric relaxation peaks take place when the hopping frequency of the localized electric charge carriers becomes approximately equal to that of the externally applied ac electric field.

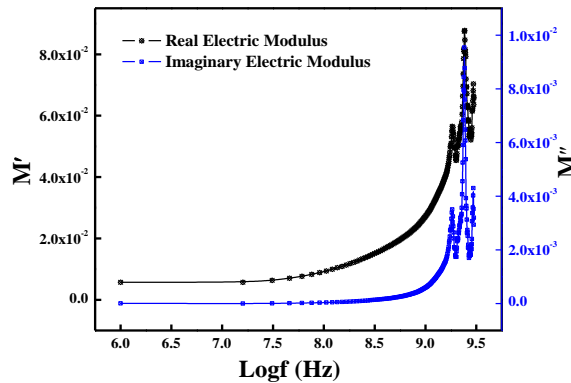


Fig. 2 Frequency dependent real and imaginary part of electric modulus.

It is obvious from the Fig. 2 that at lower frequencies the real and imaginary part of electric modulus exhibit low value which may be due to the large value of capacitance associated with the electrode polarization and at high frequency it shows high values as a consequence of low value of capacitance [33]. The ac conductivity of PANi-PSSA composite was studied and it was found to be a function of frequency as shown in Fig. 3(a). The frequency dependent ac conductivity showed a plateau in the low frequency region and dispersion at high frequency region. In the low frequency region the conductivity is independent of frequency and at high frequency, it becomes frequency dependent. The early trend in the low frequency region is due to the free charges available in the polymer matrix and the later one is due to the trapped charges which are only active at high frequency [34-36]. In case of PANi-PSSA the presence of substituent attached with the main chain of PANi may be the cause of decrease in the electrical conductivity [37]. The variation of the ac conductivity (σ_{ac}) with the frequency at room temperature shows a normal behavior, it increases with the increase of frequency. Frequency dependence of ac conductivity $\sigma(\omega)$ follows the relation [38].

$$\sigma(\omega) = A\omega^n, \quad (9)$$

Where $\omega = 2\pi f$, n is dimensionless exponent and A has the dimensions of $\Omega^{-1}\text{cm}^{-1}$. Dielectric constant and ac conduction mechanism are strongly correlated as it is introduced by Zhang *et. al.* [39].

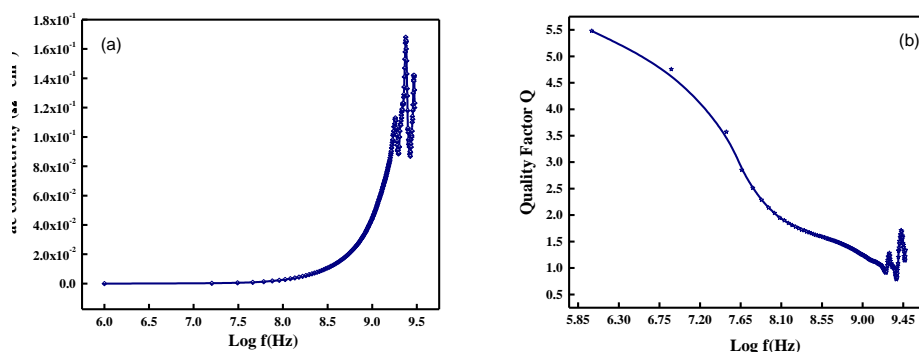


Fig. 3 Frequency dependent (a) ac conductivity and (b) quality factor of PANi-PSSA.

The quality factor ($Q = \frac{1}{\tan\delta}$) is shown in Fig. 3(b). The value of the quality factor of PANi-PSSA indicates that this material can be used in various industrial applications; as it has minimum loss value and it has comparatively high values of quality factor as compared to the rare earth doped soft ferrites [40]. The variation of resistivity with frequency is shown in Fig. 4(a). At low frequency the resistivity is high its mean the grain boundary plays an important role but as the frequency becomes high, the resistivity becomes low; so the grains play an effective role at the high frequency and resistivity decreases with the increase of frequency.

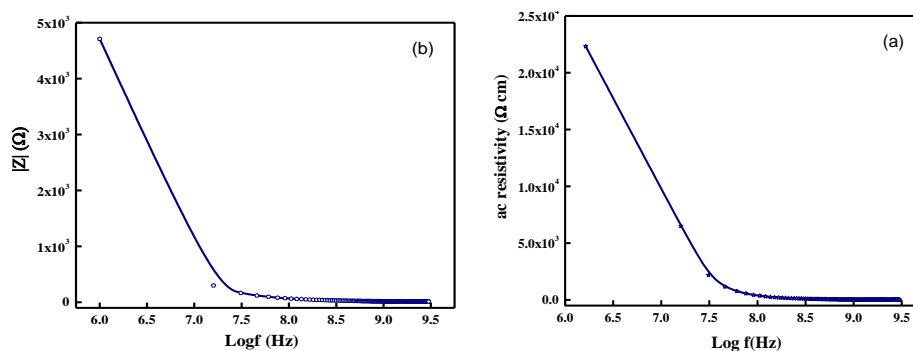


Fig. 4 Frequency dependent (a) ac resistivity and (b) Impedance.

Fig. 4(b) demonstrates impedance values that were measured at room temperature and shows a quite similar behavior as that of ac resistivity. The values of the main parameters like real dielectric constant, imaginary dielectric constant, tangent loss, ac conductivity and capacitance are given in the Table I.

Table. I. The values of different parameters at a high frequency $\log f = 9.5\text{Hz}$.

Name	ϵ'	ϵ''	$\tan \delta$	$\sigma_{ac} (\Omega^{-1}\text{cm}^{-1})$	C (PF)
PAni-PSSA	16	13	12	0.1	4.5

The capacitance value is high at low frequencies but it is low at high frequencies as shown in Fig. 5. In fact, the alternating voltage half period becomes shorter at high frequencies so the space charge polarization fails to settle itself and capacitance begins to drop. The time required for electronic or ionic polarization to set in is very small as compared with the time of voltage sign change between the two half-period of the applied alternating voltage. The variation of capacitance with frequency is given by the relation [41],

$$C = C_g + [s\tau/(\omega^2\tau^2 + 1)], \quad (10)$$

Where C_g is geometrical capacitance, s is conductance corresponding to absorption current, τ is the dipole relaxation time and ω is the angular frequency. According to this, capacitance is maximum when $\omega = 0$ and minimum when $\omega = \infty$ [42].

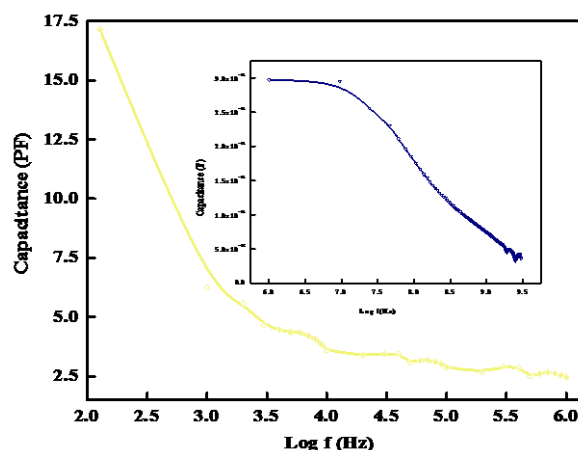


Fig. 5 Dynamical change in capacitance versus $\log f$ (Hz). Inset shows the capacitance versus $\log f$ (Hz) at higher frequency i.e. 1MHz to 3 GHz range.

3.2 Temperature dependent electrical properties of PAni-PSSA

In case of temperature dependence capacitance, the decrease in capacitance after the peak may be due to the decrease in the order of the oriented polarized charges [43-44]. If the voltage across a dielectric material is increased steadily then on the appearance of any imperfections in the material or its surrounding will cause a breakdown in the material. The quick release of so much high energy at a high voltage usually means that the material burns out in the breakdown region between the electrodes. The molecular chain rings in the structure of PAni-PSSA show a sharp line-width transition at about 60 °C, which is attributed to the dielectric breakdown as shown in Fig. 6(a).

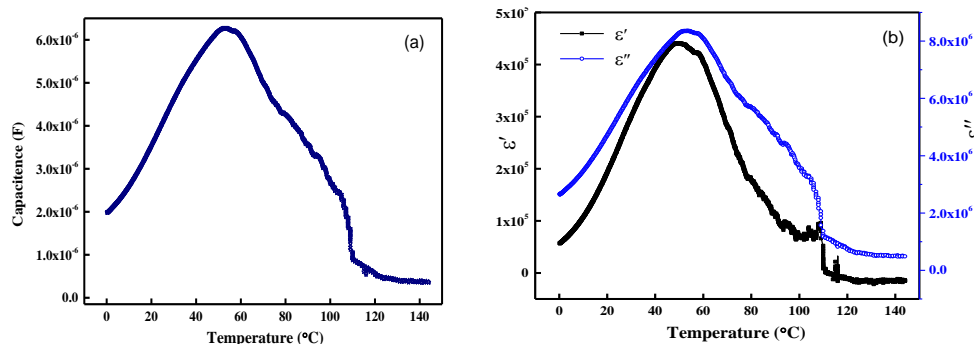


Fig. 6 Temperature dependent (a) capacitance and (b) real and imaginary dielectric constant of PANi-PSSA.

After the dielectric breakdown the hopping of the molecules takes place. Dielectric breakdown is usually associated with a localized flaw and is not considered as a whole representative of the material. The dipoles become free with the rise of temperature and respond rapidly to the electric field. The increase in dielectric constant with temperature is due to the greater free movement of dipole molecular chain of PANi-PSSA [see Fig. 6(b)]. At low temperature the dipoles are rigidly fixed in the material and are not in the position to change their orientation. The tangent loss is shown in Fig. 7(a), the dispersion peaks nearby 90°C are due to the evaporation of absorbed water. The temperature dependent electrical conductivity follows the Arrhenius rule. The charge transport can be expressed by the Arrhenius relation [44].

$$\sigma_T = \sigma_0 \exp\left(-\frac{\Delta E}{kT}\right) \quad (11)$$

Where σ_0 is a constant, ΔE the activation energy, k the Boltzmann constant and T is the temperature. The value of activation energy ($\Delta E = 0.1 \text{ eV}$) is taken from the slope of $\ln(\sigma)$ versus $\frac{1}{T}$, from Fig. 7(b). It is clear from the activation energy that the conduction mechanism may be due to the hopping of electrons.

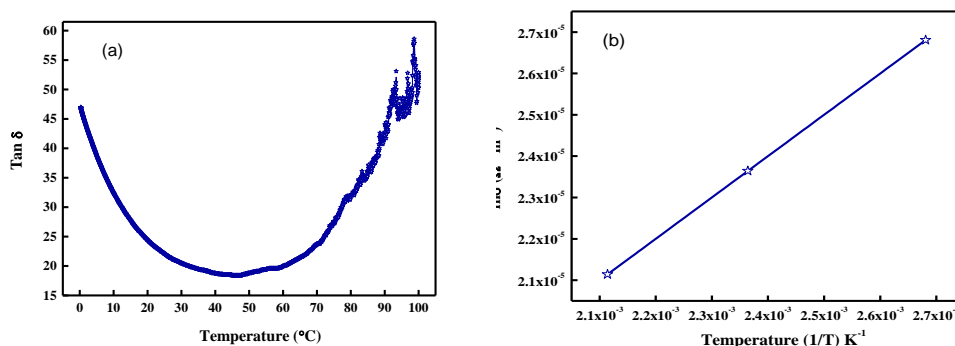


Fig. 7 Temperature dependent (a) $\tan \delta$ and (b) $\ln \sigma$ versus inverse of temperature.

Thermogravimetric analysis (TGA) and the derivative of weight loss (DTG) for PANi-PSSA are shown in Fig. 8(a). It is clear from the DTG curve of PANi-PSSA three significant events takes place. The initial event show the decomposition due to water or moisture evaporation up to 140 °C, a second event is the decomposition in the range 140 °C to 250 °C, it is due to oligomer and in the last event major weight loss after 425 °C is due to the decomposition of polymer. The same behavior is reported in the literature by G. Neetika *et. al.* [45-46].

Fig. 8(b) demonstrates the Fourier transform infrared (FTIR) absorbance spectrum of PANi-PSSA. The peaks at 1608 cm^{-1} and 1406 cm^{-1} corresponds to the C=C stretching deformation of quinoid and benzenoid rings, respectively. The peak at 1130 cm^{-1} is due to C-N stretching of

secondary amine while the absorption at 842 cm^{-1} is assigned to the out of plane deformation of C-H in the 1,4-disubstituted benzene ring. Moreover, the peak at 1009 cm^{-1} ascribed to $-\text{SO}_3^-$ group was also observed in the spectrum of the soluble PAni-PSSA. All these show that PAni has been successfully obtained and PSSA has been incorporated into the soluble product [47].

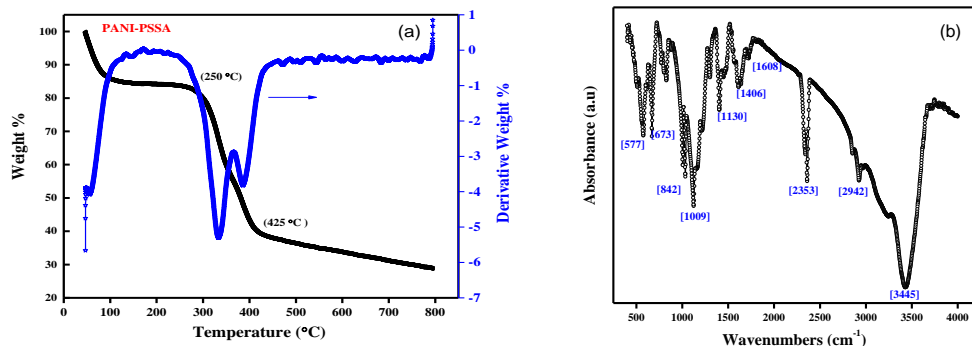


Fig.8(a) TGA/DSC curve and (b) FTIR absorbance spectrum of PAni-PSSA.

4. Conclusions

FTIR spectrum of synthesized composite PAni-PSSA confirms the existence of conductive polyaniline. The ac conductivity showed a plateau in the low frequency region and dispersion at the high frequency region. The dispersion of ac conductivity is explained on the basis of Maxwell-Weigner and Koops model. The increase in ac conductivity was due to the creation of additional hopping sites in the polymeric composite. The high value of dielectric constant of PAni-PSSA is due to its thinner walls of the grain boundaries. The material PAni-PSSA follows the Arrhenius relation, it shows that the material is semiconductor and reflects the hopping of electrons. The value of the real and imaginary dielectric constant are increasing with temperature due to greater freedom movement of the dipoles of PAni-PSSA molecular chain and the dielectric breakdown takes place at $60\text{ }^{\circ}\text{C}$. The variation of ac conductivity with frequency shows that the electrical conduction is mainly due to electron hopping. On the basis of these properties, it is suggested that the composite may be suitable for switching, dielectric material in capacitors, humidity sensing and in microwave devices.

References

- [1] H. Shirakawa, E. J Louis, A. G, Mac Diarmid, C. K Chiang, A. J Heeger, J. Chem. Soc. Chem. Commun. **16**, 578 (1977).
- [2] J. Jang, Y. Nam, H. Yoon, Adv. Mater. **17**, 1382 (2005).
- [3] T. M. Wu, S. H Lin, J. Pol. Sc. A **44**, 6449 (2006).
- [4] N. Gupta, D. Kumar, S. K. Tomar, Int. J. of Mater. and Chem. **2**(2), 79 (2012).
- [5] C. S. Stan, M. Popa, M. Olariu, M. S. Secula, Open Chem. **13**, 467 (2015).
- [6] B. Kim, V. Koncar, E. Devaux, AUTEX Research Journal. **4**(1), 9 (2004).
- [7] C. P. Chwang, C. D. Liu, S. W. Huang, D. Y. Chao, S. N. Lee, Syn. Met. **142**, 275 (2004).
- [8] A. Imani, G. Farzi, A. Ltaief, Facile Int. Nano. Lett. **3** 52 (2013).
- [9] H. Letheby, J. Chem. Soc. **224**, 161 (1862).
- [10] M. E. Goppelsroder. Compt. Rend. **82**, 331 (1876).
- [11] J. C. Chiang, A. G. MacDiarmid, Synth. Met. **13**, 193 (1986).
- [12] C. Lucignano, F. Quadrini, L. Santo, J. of Comp. Materials. **42**, 2841 (2008).
- [13] L. H. Abound, Natural and Applied Sciences. **4**, 73 (2013).
- [14] N. G, McCrum B E, Read Williams G. Wiley, (London) (1967).
- [15] M. A. El-Shahawy, A. F. Mansour, H. A. Hashem, J. Pure Appl. Phys. **36**, 78 (1998).

- [16] C. J. F. Böttcher, P. Bordewijk, Theory of dielectric polarization, Elsevier (Amsterdam), (1973).
- [17] M. Cook, D. C. Watts, G. Williams, Trans. Faraday Soc. **66**, 2503 (1970).
- [18] N. E. Hill, W. E. Vaughan, A. H. Price, M. Davis, Dielectric Properties and Molecular Behaviour, Van Nostrand(London), (1969).
- [19] C. F. Böttcher, P Scaife, Principles of Dielectrics Oxford University Press (Oxford), (1989).
- [20] K. S. Lee, G. B. Blanchet, F. Gao, Y. L. Loo, Appl. Phys. Lett. **86**, 074102 (2005).
- [21] J. C. Maxwell, A. Treatise on electricity and Magnetism, Oxford, New York 2, (1954).
- [22] K. W. Wagner, Ann. Phys. **40**, 817 (1913).
- [23] C. G. Koops, Phys. Rev. **83**, 121 (1951).
- [24] S. Kazan, E. E. Tanriverdi, R. Topkaya, S. Demirci, O. Akman, A. Baykal, B. Aktas, J. Chem. **9**, 2440 (2012).
- [25] S. V. Jadhav, V. Puri, Synth. Met. **158**, 883 (2008).
- [26] S. M. Reda, Dyes Pigments **75**, 526 (2007).
- [27] F. Latif, M. Aziz, N. Katun, M. Ali, M. Z. A. Yahya, J. Power Sources. **1594**, 1401 (2006).
- [28] S. Havriliak, S. Negami J. Polym. Sci. Part-C. **14**, 99 (1966).
- [29] J. C. Maxwell, Electricity and Magnetism, Oxford University Press, London 1, (1873).
- [30] B. A. Afzal, M. J. Akhtar, M. Nadeem, M. M. Hassan, J. Phys. Chem. C **113**, 17560 (2009).
- [31] B. Zhou, Y. W. Zhang, C. S. Liao, F. X. Cheng, C. H. Yan, J. of Mag. and Mag. Materials **247**, 70 (2002).
- [32] G. Murtaza, I. Ahmad, A. Hakeem, P. Mao, X. Guohua, Digest J. Nanomater. Biostructures **11**(2), 477 (2016).
- [33] S. Fang, C. H. Ye, T. Xie, Z. Y. Wong, J. W. Zhao, L. D. Zhang, Appl. Phys. Lett. **88**, 013101 (2006).
- [34] S. B. Aziz, Z. H. Z. Abidin, A. K. Arof, Express Polymer Letter **4**(5), 300 (2010).
- [35] H. P. de Oliveira, M. V. B. dos Santos, C.G. dos Santos, C. P. de Melo, Mater. Charact. **50**, 223 (2003).
- [36] H. P. de Oliveira, M. V. B. dos Santos, C. G. dos Santos, C. P. de Melo, Synth. Met. **135**, 447 (2003).
- [37] P. B. Macedo, C. T. Moynihan, R. Bose, Phys. Chem. Glasses. **13**, 171 (1972).
- [38] M. T. Ramesan, Polymer Plastic Technology and Engineering **51**, 1223 (2012).
- [39] Z. Kezhao, Fredkin, R. Donald, J Appl. Phys. **85**, 6187 (1999).
- [40] E. Ateia, M. A. Ahmed, A. K. El-Aziz, J. Magn. Mag. Mater. **311**, 545 (2007).
- [41] G. Murtaza, I. Ahmad, J. Wu, Mater. Sc. in Semicond. Process. **34**, 269 (2015).
- [42] C. Corbella, M. Vives, A. Pinyol, I. Porqueras, C. Person, E. Bertran, Sol. State Ionic. **15**,165 (2003).
- [43] M. S. Mattsson, G. A. Niklasson, J. Appl. Phys. **85**, 8199 (1999).
- [44] C. M. Keum, J. H. Kwon, S. D. Lee, J. H. Bae, Solid State Electronics. **89**, 189 (2013).
- [45] N. Gupta, D. Kumar, S. K. Tomar, Int. J. of Materials and Chem. **2**(2), 79 (2012).
- [46] Q. M. Jia, S. Y. Shan, Y. M. Wang, Poly. Mater. Sc. and Engg. **9**, 159 (2010).
- [47] Y. Li, B. Ying, L. Hong, M. Yang, Syn. Met. **160**, 455 (2010).